Journal of Power Sources 188 (2009) 141–147

Contents lists available at ScienceDirect

Journal of Power Sources

journal homepage: www.elsevier.com/locate/jpowsour

Degradation of proton exchange membrane fuel cells due to CO and CO_2 poisoning

Wei-Mon Yan[a,*], Hsin-Sen Chu[b], Meng-Xi Lu[b], Fang-Bor Weng[c], Guo-Bin Jung[c], Chi-Yuan Lee[c]

[a] Department of Mechatronic Engineering, Huafan University, Taipei 223, Taiwan
[b] Department of Mechanical Engineering, National Chiao Tung University, Hsin-Chu 300, Taiwan
[c] Department of Mechanical Engineering, Fuel Cell Center, Yuan Ze University, NeiLi, Taoyuan 320, Taiwan

ARTICLE INFO

Article history:
Received 22 October 2008
Received in revised form
24 November 2008
Accepted 24 November 2008
Available online 6 December 2008

Keywords:
PEM fuel cell
CO poisoning
CO_2 poisoning
Degradation of cell performance

ABSTRACT

The CO and CO_2 poisoning effects on the degradation of cell performance of proton exchange membrane fuel cell (PEMFC) under transient stage were investigated. The mechanism of CO poisoning lies in the preferential adsorbing of CO to the platinum surface and the blocking of active sites of hydrogen. These phenomena were described with adsorption, desorption, and electro-oxidation processes of CO and hydrogen in the present work. In addition, it is well known that the reverse water gas shift reaction (RWGS) is the main effect of the CO_2 poisoning, through which a large part of the catalytic surface area becomes inactive due to the hydrogen dissociation. The predicted results showed that, by contaminating the fuel with 10 ppm CO at the condition of $P_H = 0.8$ atm and $P_{CO_2} = 0.2$ atm, the current density of the PEM fuel cell was lowered 28% with rate constant of RWGS k_{rs} from zero to 0.02. With 50 ppm CO, the performance drop was only 18%. For the reformed gas, CO_2 poisoning became much more significantly when the CO content in the reactant gas was small.

1. Introduction

Nowadays, hydrogen production from fossil fuel is one of present common ways, and is usually realized through such methods as steam reforming, partial oxidation and autothermal reforming. However, gas produced from reformer contains about 70–75% hydrogen, 20–25% carbon dioxide and also 10–100 ppm carbon monoxide. Fuel cell performance would be attenuated if the carbon monoxide concentration reaches to 5–10 ppm [1,2]. The mechanism of CO poisoning lies in the preferential adsorbing of CO to the platinum surface and the blocking of active sites of hydrogen [3]. Platinum is still the best catalyst layer for PEM fuel cell, however the operating temperature is about 60–100 °C in which the carbon monoxide absorption on the platinum catalyst layer would cause attenuation of the fuel cell performance. To improve CO tolerance of fuel cells, alloys are ordinary catalytic medium while Pt–Ru alloys are the most common catalytic medium for PEMFC as commercial fuel cells since Pt–Ru has better CO tolerance.

Gastiger et al. [4] concluded that the best mixing ratio of the Pt–Ru alloys is 1:1. Yu et al. [5] experimentally studied the structure of the Pt–Ru alloys. They used the inner and outer catalyst layers to make a complete catalyst layer. The experimental results showed that this composite structure provides a higher CO tolerance than traditional catalyst layer of the Pt–Ru alloys. Santiago et al. [6] dispersed Ru onto the diffusion layer and having CO oxidized to CO_2 before reaching catalyst layer. However the application of noble metal resulted in the increase in the cost. Therefore, part of researchers focused on how to resume the fuel cell performance after being poisoned by CO. Commonly aimed at CO oxidation, there are three methods as follows: oxidant-bleeding [7–11], self-oxidation [1,12] and current-pulsing [12–14].

Springer et al. [15] developed a CO poisoning model and described the effects of catalyst layer adsorption, desorption and electrochemical reaction when anode feed stream consisted of H_2 and CO. The surface area of the catalyst layer differed with time due to the cover of H_2 and CO, consequently influenced the cell performance. In 2003, Chan et al. [16] proposed a mathematical model of polymer electrolyte fuel cell with different CO concentration, gas concentration cover ratio in steady state. Bhatia and Wang [17] extended Springer's model [15] and investigated influence of CO on fuel cell performance. In their model, Bhatia and Wang neglected the current density produced by CO as well as the thickness effect of catalyst layer. Liu and Zhou [18] employed CFD software to investigate the influence of CO poisoning on the cell performance of the PEM fuel. Chu and his co-workers [19] developed both single and two-phase flow model to analyze the transient CO poisoning process of the PEM fuel cell. Wang et al. [20] further investigated the CO poisoning effect on the high temperature PBI membrane fuel cell.

Bruijn et al. [21] further discussed the influence of CO_2 poisoning on cell performance and the results showed that the Pt–Ru alloys as catalyst layer had a better CO_2 tolerance when the temperature

* Corresponding author. Tel.: +886 2 2663 2102; fax: +886 2 2663 1119.
E-mail address: wmyan@cc.hfu.edu.tw (W.-M. Yan).

0378-7753/$ – see front matter © 2008 Elsevier B.V. All rights reserved.
doi:10.1016/j.jpowsour.2008.11.107

Nomenclature

a	surface area per unit catalyst layer volume ($cm^2\ cm^{-3}$)
B_i	Tafel slope of species i (V)
$b_{i,ads}$	desorption rate constant of species i (atm)
C_i	concentration of species i ($mol\ cm^{-3}$)
D_i	diffusion coefficient of species i ($cm^2\ s^{-1}$)
ΔE_H	activation energy of hydrogen ($J\ mol^{-1}$)
F	Faraday constant ($C\ mol^{-1}$)
ΔG_{CO}	Gibbs free energy of carbon monoxide ($J\ mol^{-1}$)
i	current density ($A\ cm^{-2}$)
I	operating current density ($A\ cm^{-2}$)
$k_{i,ads}$	adsorption rate constant of species i ($A\ cm^{-2}\ atm^{-1}$)
$k_{i,ox}$	electrochemistry reaction rate constant of species i ($A\ cm^{-2}$)
k_{rs}	rate constant of reverse water gas shift reaction ($A\ cm^{-2}\ atm^{-1}$)
n_i	electron number of species i
P	pressure (atm)
R	universal gas constant ($J\ mol^{-1}\ K^{-1}$)
r	interaction parameter of carbon monoxide ($J\ mol^{-1}$)
s_i	stoichiometric number of species i
T	temperature (K)
t	time (s)
V_0	open loop voltage (V)
V	voltage (V)
X	mole fraction
z	axial coordinate (μm)

Greek letters

α	transport coefficient
β	symmetry factor of CO adsorption
ε	porosity
ρ	product of the catalyst layer surface density and Faraday constant ($C\ cm^{-2}$)
λ	influence area per unit CO
θ_i	fraction of the catalytic surface area covered by species i
ϕ	voltage (V)
η	overvoltage (V)
κ	proton transport coefficient ($m\Omega\ cm^{-1}$)
σ	electron transport coefficient ($m\Omega\ cm^{-1}$)

Superscripts

0	initial value
c	catalyst layer
in	catalyst layer inlet

Subscripts

0	initial value
a	anode
c	cathode
i	H_2 or CO
ss	steady state

was increased. Since then, Janssen [22] added CO_2 poisoning model into the CO poisoning model and assumed that the reverse water gas shift reaction (RWGS) is the reason of the CO_2 poisoning effects. The results showed that CO_2 poisoning would have the significant effect when the CO content is small and at relatively low operating current density. At high operating current density, CO would be the dominating poisoning gas. Dhar et al. [23] developed a series of empirical correlations to determine the CO coverage in fuel cell

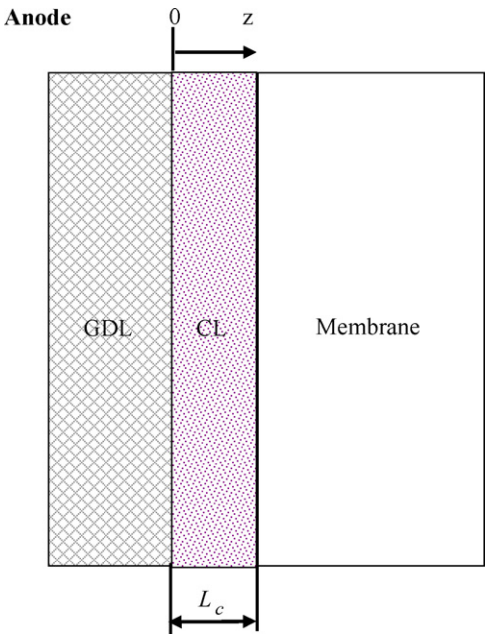

Fig. 1. Schematic diagram of the physical model.

and mainly investigated the influence of CO poisoning on phosphate fuel cell performance at various temperature as well as various CO concentrations. They found that CO coverage would have a liner relationship with $\ln[CO]/[H_2]$ at various temperature. Batisa et al. [24] applied water gas shift reactor and methanation reactor to slow down CO poisoning and both these two reactors had a significant relationship with CO_2.

According to previous research, although there are studies on CO or CO_2 poisoning of fuel cell, still lack of investigation on combined CO and CO_2 poisoning on the degradation of cell performance of PEM fuel cell at transient time. This motivates the present study. In this work, both CO and CO_2 poisoning were combined to examine the transient degradation of cell performance and the significance of CO_2 poisoning.

2. Analysis

The physical model of this work is shown schematically in Fig. 1. The purpose of this study is to investigate the unsteady behaviors of hydrogen concentration, carbon monoxide concentration, platinum surface coverage and the current density distributions after anode catalyst layer of PEM fuel cell being poisoned by CO and CO_2. Due to the main influence area of CO poisoning being on the anode catalyst layer, therefore, the examined domain is fixed on anode catalyst layer. Origin is set on the interface between anode gas diffusion layer and anode catalyst layer ($z = 0$). Since catalyst layer thickness is far less than the catalyst layer length (width), so it could be considered as one-dimensional system. To simplify the analysis, the following assumptions are made:

1. The system is one-dimensional Cartesian coordinate system.
2. The species are ideal gas.
3. The catalyst layer is porous medium with uniform porosity.
4. Only diffusion transport is considered in the catalyst layer.
5. Anode overvoltage is assumed to be constant.

With the above assumptions, the governing equations are described as follows:

$$H_2: \quad \varepsilon_c \frac{\partial C_{H_2}}{\partial t} = \varepsilon_c D_{H_2} \frac{\partial^2 C_{H_2}}{\partial z^2} - \frac{di_{H_2}}{dz}\left(\frac{s_{H_2}}{n_{H_2} F}\right) \tag{1}$$

$$\text{CO}: \quad \varepsilon_c \frac{\partial C_{\text{CO}}}{\partial t} = \varepsilon_c D_{\text{CO}} \frac{\partial^2 C_{\text{CO}}}{\partial z^2} - \frac{di_{\text{CO}}}{dz}\left(\frac{s_{\text{CO}}}{n_{\text{CO}}F}\right) \tag{2}$$

where the first term in both Eq. (1) or Eq. (2) stands for the concentration variation with time in control volume, while the second term means the concentration variation rate due to diffusion and the third term is concentration consumption rate caused by electrochemical reaction.

If hydrogen, carbon monoxide and carbon dioxide exist on anode catalyst layer at the same time, adsorption, desorption and electrochemical reaction would happen between H_2/CO and platinum surface of catalyst layer which consequently affect the coverage of H_2/CO on platinum surface. Meanwhile, CO_2 would start reverse water gas shift reaction and cause the adsorbed H_2 desorbed from the platinum catalyst layer. All these electrochemical reaction rates depend on each reaction rate constant and the coverage governing equations are as follows:

$$\rho\frac{d\theta_{\text{H}}}{dt} = k_{\text{H},ads}X_{\text{H}_2}P\left(1-\theta_{\text{H}}-\theta_{\text{CO}}\right) - b_{\text{H},ads}k_{\text{H},ads}\theta_{\text{H}} - k_{\text{rs}}X_{\text{CO}_2}P\theta_{\text{H}}^2 - 2k_{\text{H},ox}\theta_{\text{H}}\sinh\left(\frac{\eta_a}{B_{\text{H}_2}}\right) \tag{3}$$

$$\rho\frac{d\theta_{\text{CO}}}{dt} = k_{\text{CO},ads}X_{\text{CO}}P\left(1-\theta_{\text{H}}-\theta_{\text{CO}}\right)\exp\left(-\frac{\beta r\theta_{\text{CO}}}{RT}\right) - b_{\text{CO},ads}k_{\text{CO},ads}\theta_{CO}\exp\left(-\frac{\left[1-\beta\right]r\theta_{\text{CO}}}{RT}\right) + k_{\text{rs}}X_{\text{CO}_2}P\theta_{\text{H}}^2 - 2k_{\text{CO},ox}\theta_{\text{CO}}\sinh\left(\frac{\eta_a}{B_{\text{CO}}}\right) \tag{4}$$

The term of the left side in Eq. (3) or Eq. (4) stands for rate of coverage, for the right side, the first term means for the increased rate of absorbed H_2/CO, the second term is decreased rate of desorbed H_2/CO, the third term means the rate of desorbed H_2 caused by RWGS, and the fourth term means consumption rate caused by electrochemical reaction. The correction made by Li and Baschuk [10] was adopted for the first and second terms of right side in Eq. (4).

In addition, Springer et al. [15] found that H_2 adsorption rate constant and CO desorption rate constant had a relationship with the CO coverage on catalyst surface, the relationship are given by [15]:

$$k_{\text{H},ads} = k_{\text{H0},ads}\exp\left[-\frac{\delta(\Delta E_{\text{H}})}{RT}\left(1-\exp\left(\frac{\lambda\theta_{\text{CO}}}{\theta_{\text{CO}}-1}\right)\right)\right] \tag{5}$$

$$b_{\text{CO},ads} = b_{\text{CO0},ads}\exp\left[\frac{\delta(\Delta G_{\text{CO}})}{RT}\theta_{\text{CO}}\right] \tag{6}$$

Due to the CO poisoning effect, H_2 and CO molecules exist on the catalyst layer surface, therefore, the generated current density caused by electrochemical reaction are mainly produced by H_2 and CO. Therefore, the standard Bulter–Volmer equation must be corrected on platinum surface coverage, and the modified equation is given as

$$\frac{di}{dz} = \frac{di_{\text{H}_2}}{dz} + \frac{di_{\text{CO}}}{dz} = 2ak_{\text{H},ox}\theta_{\text{H}}\sinh\left(\frac{n_{\text{H}_2}\eta_a}{B_{\text{H}_2}}\right) + 4ak_{\text{CO},ox}\theta_{\text{CO}}\sinh\left(\frac{n_{\text{CO}}\eta_a}{B_{\text{CO}}}\right) \tag{7}$$

where the parameter, a, stands for the surface area per unit catalyst layer, while the first term in right side stands for the generated current density from H_2-electrochemical oxidation, the second term is the generated current density from CO-electrochemical oxidation.

Table 1
Values of the basic parameters used in this work.

Parameter	Value
T, temperature (K)	353
P, pressure (atm)	3
α, transfer coefficient	0.5
D_{H_2}, diffusion coefficient of H_2 ($\text{cm}^2\ \text{s}^{-1}$)	2.59×10^{-6}
D_{CO}, diffusion coefficient of CO ($\text{cm}^2\ \text{s}^{-1}$)	5.4×10^{-7}
B_{H_2}, Tafel slope of H_2 electro-oxidation reaction (V)	0.032 [13]
B_{CO}, Tafel slope of CO electro-oxidation reaction (V)	0.06 [13]
β, symmetry factor of CO adsorption	0.1 [8]
r, interaction parameter of CO (J mol^{-1})	39.7 [8]
$k_{\text{H}_2\text{O},ads}$, adsorption rate constant of H_2 ($\text{A cm}^{-2}\ \text{atm}^{-1}$)	100
$b_{\text{H}_2,ads}$, desorption rate constant of H_2 (atm)	0.5 [15]
$k_{\text{H}_2,ox}$, electrochemistry reaction rate constant of H_2 (A cm^{-2})	4 [15]
$k_{\text{CO},ads}$, adsorption rate constant of CO ($\text{A cm}^{-2}\ \text{atm}^{-1}$)	10 [15]
$b_{\text{CO0},ads}$, desorption rate constant of CO (atm)	1.51×10^{-9}
$k_{\text{CO},ox}$, electrochemistry reaction rate constant of CO (A cm^{-2})	1×10^{-8} [13]
k_{rs}, rate constant for reverse water gas shift reaction ($\text{A cm}^{-2}\ \text{atm}^{-1}$)	0.02 [18]

In this work, to simplify the analysis, the PEM fuel cell was assumed to initially keep in a non-operating state. This means that when $t=0$, there is no reactant gas in the fuel cell and when $t>0$, the reactant gas starts to flow into the fuel cell. Therefore, the initial conditions are given by

$$C_{\text{H}_2}(z,0) = C^0_{\text{H}_2}(z,0) \tag{8}$$

$$C_{\text{CO}}(z,0) = C^0_{\text{CO}}(z,0) \tag{9}$$

$$\theta_{\text{H}}(z,0) = \theta^0_{\text{H}} \tag{10}$$

$$\theta_{\text{CO}}(z,0) = \theta^0_{\text{H}} \tag{11}$$

For the concentration boundary conditions, fixed values of species at $z=0$ were assumed:

$$z=0: \quad C_{\text{H}_2} = C^{in}_{\text{H}_2}, \quad C_{\text{CO}} = C^{in}_{\text{CO}} \tag{12}$$

while at the interface between catalyst layer and membrane ($z=L_c$), due to the gas blocking effect of membrane, concentration fluxes of species were set to be zero:

$$z=L_c: \quad D_{\text{H}_2}\frac{\partial C_{\text{H}_2}}{\partial z} = 0, \quad D_{\text{CO}}\frac{\partial C_{\text{CO}}}{\partial z} = 0 \tag{13}$$

For the condition of current density, the current density at $z=0$ is assumed to be zero:

$$z=0: \quad i=0 \tag{14}$$

3. Solution method

According to the assumptions, the governing equations, boundary conditions and initial conditions discussed in the previous sections, coupling with the parameters in Table 1, are non-linear and are difficult to get the analytical solution. In this work, the control volume finite difference method is adopted to solve the non-linear, coupled ordinary differential equations. The detailed solution scheme is available in Ref. [25]. In addition, the Crank–Nicolson and Runge–Kutta methods are employed to solve for the concentration equations and the coverage equation of the catalyst layer, respectively.

To check the grid independence, solutions on various grid systems are examined. It is found in the separate numerical runs that there is not any difference among the solutions with three grid arrangements: 500, 1000 and 2000 points. In order to save the calculating time, 500 grids are adopted for the present problem. Additionally, it is important to compare the predicted results with existing experimental data. It is apparent that the present predictions agree well with those of Oetjen et al. [26]. Through these

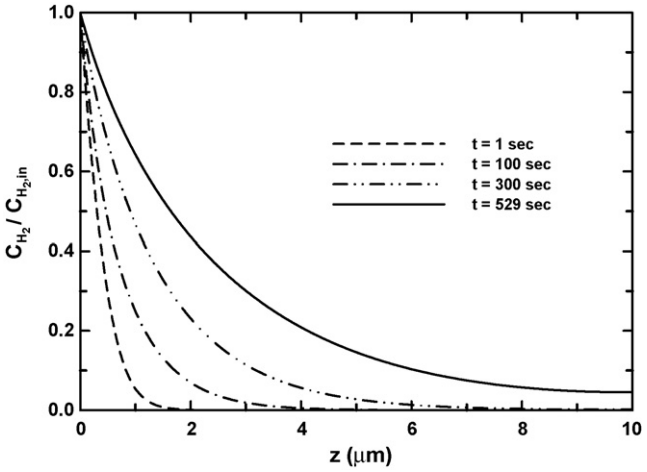

Fig. 2. The transient evolution of H_2 distribution across the catalyst layer with 100 ppm CO.

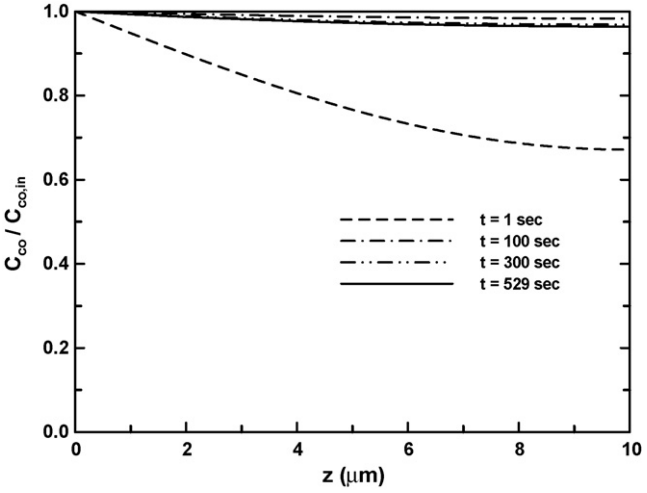

Fig. 3. The transient evolution of CO distribution across the catalyst layer with 100 ppm CO.

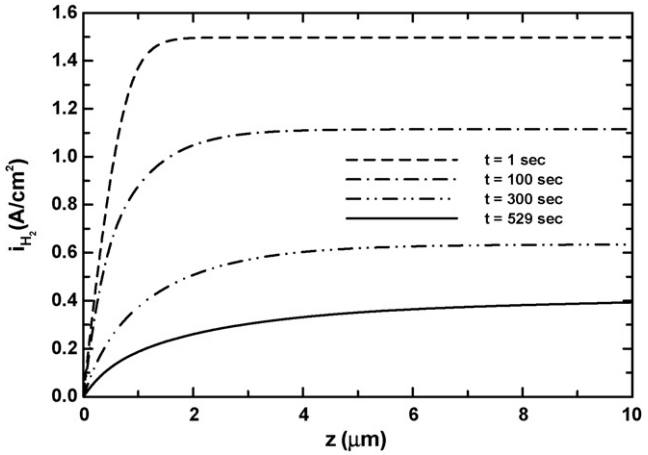

Fig. 4. The transient evolution of current density distribution across the catalyst layer induced by H_2 with 100 ppm CO.

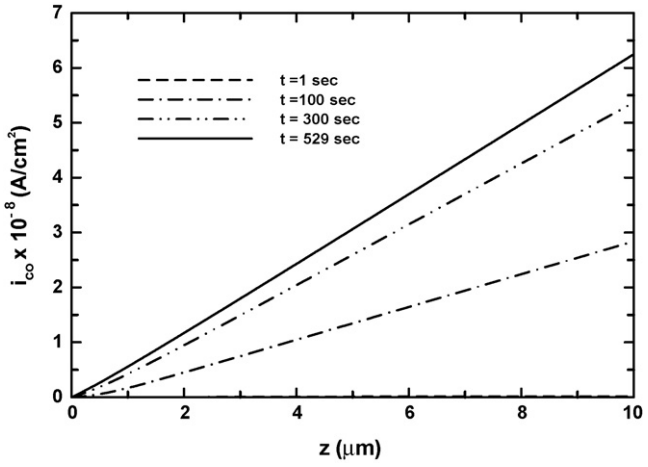

Fig. 5. The transient evolution of current density distribution across the catalyst layer induced by CO with 100 ppm CO.

preliminary tests, it is found that the numerical method is suitable for the present study.

4. Results and discussion

When the PEM fuel cell starts up, the cell performance would decay if the reactant gas contains a certain amount of CO. With the concentration of 100 ppm CO in the hydrogen of anode fuel, the coverage of the platinum will be changed. This is because the CO is easier to combine with the platinum to form a steady bond, which is difficult to electrolyze to generate the current. The surface of platinum would be covered by the accumulating CO, leading to the decreasing of current density generated by the hydrogen. As indicated in Figs. 2 and 3, CO would struggle for the catalyst by competing with hydrogen as soon as it contacts with the catalyst layer. The quantity of CO adhering on the platinum surface lies on the diffusion velocity and the concentration when it goes through the catalyst layer. In addition, the consuming rate of hydrogen would be slowed with the decreasing reaction area between hydrogen and catalyst layer. The excessive hydrogen would diffuse to the boundary between the catalyst layer and the membrane, looking for a reactivity region. By contraries, CO is absorbed by the platinum surface and does not participate. Therefore, the consuming rate of CO is very limited, leading to the accumulation of CO on the catalyst layer, as shown in Fig. 3.

Figs. 4 and 5 present the transient evolution of current density distributions across the catalyst layer induced by H_2 and CO with 100 ppm CO, respectively. A close examination of Figs. 4 and 5 reveals that the generated current density from CO-electrochemical oxidation could be neglected as compared to that from H-electrochemical oxidation. Therefore, the fuel cell current density was mainly produced from H_2 electrochemical reaction and current density generated from CO-electrochemical reaction would be neglected in later discussion. In other words, once H_2/Pt reaction surface area decreased, the fuel cell current density would decrease. Coverage is an important parameter for investigating the effect of CO poisoning on cell performance of PEM fuel cell. It is clearly seen in Fig. 4 that when PEM fuel cell is being poisoned by 100 ppm CO, the consequent current density dropped from 1.497 A cm^{-2} to 0.393 A cm^{-2}, dropping about 73.76%. In addition, time required for reaching steady state was prolonged from 1 s to 529 s for competing platinum surface. In the CO poisoning process, time required for reaching steady state would be affected by the change of coverage which mainly depends on CO concentration and diffusion rate on catalyst surface. Since the diffusion rate of CO is relatively slow, much more time would be needed to reach catalyst layer surface. However, once contacted onto catalyst layer, CO would have a sta-

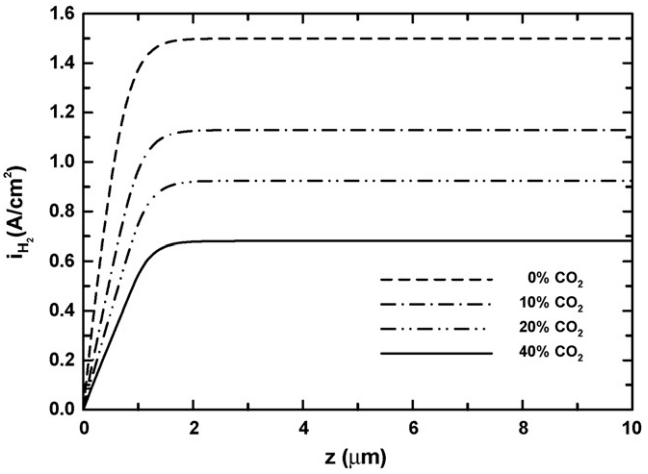

Fig. 6. The steady-state current density distribution across the catalyst layer induced by H_2 with various CO_2 concentrations.

ble connection with platinum and then gradually accumulated on the platinum surface.

Above investigation just focused on the effect of CO poisoning on cell performance, further discussion will examine the effect of CO_2 poisoning on the characteristics of PEM fuel cell through reverse water gas shift reaction. For various CO_2 concentrations, Fig. 6 shows steady-state current density distributions after PEM fuel cell being poisoned by CO_2 for the condition of 0 ppm CO concentration. With increasing CO_2 concentration, poisoning effect was getting serious. When CO_2 concentration was 10% or 40%, the current density would drop 24.69% or 54.6%.

Fig. 7 presents the steady-state current density distributions across the catalyst layer induced by H_2 with various gas combinations of reactant gases. When CO concentration is 0 ppm and rate constant of reverse water gas shift reaction k_{rs} is zero ($k_{rs} = 0$), the existence of CO_2 only has a dilution effect on fuel gas. However, for the case of $k_{rs} = 0.02$, besides the dilution effect, the CO_2 also has poisoning effect which made the cell performance dropped from 1.21 A cm^{-2} to 0.835 A cm^{-2}, about 31% decrease. Therefore, the CO_2 poisoning will be affected by the rate constant of reverse water gas shift reaction k_{rs}.

Fig. 8 shows that the transient evolutions of the H_2 coverage, CO coverage and current density in catalyst layer when the CO concentration and k_{rs} were 20 ppm and 0.02, respectively. A

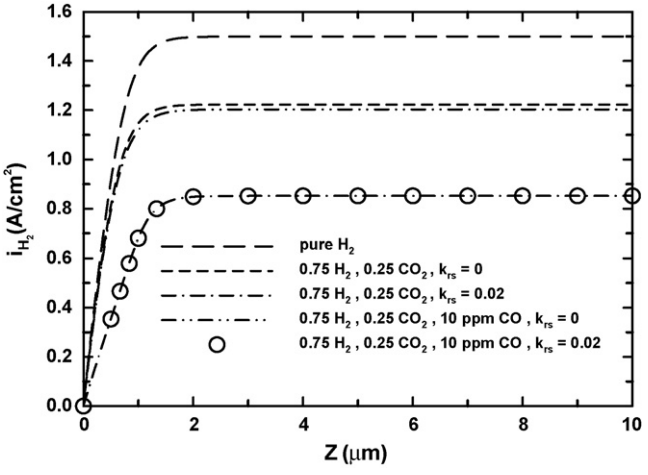

Fig. 7. The steady-state current density distribution across the catalyst layer induced by H_2 with various gas combinations of reacting gases.

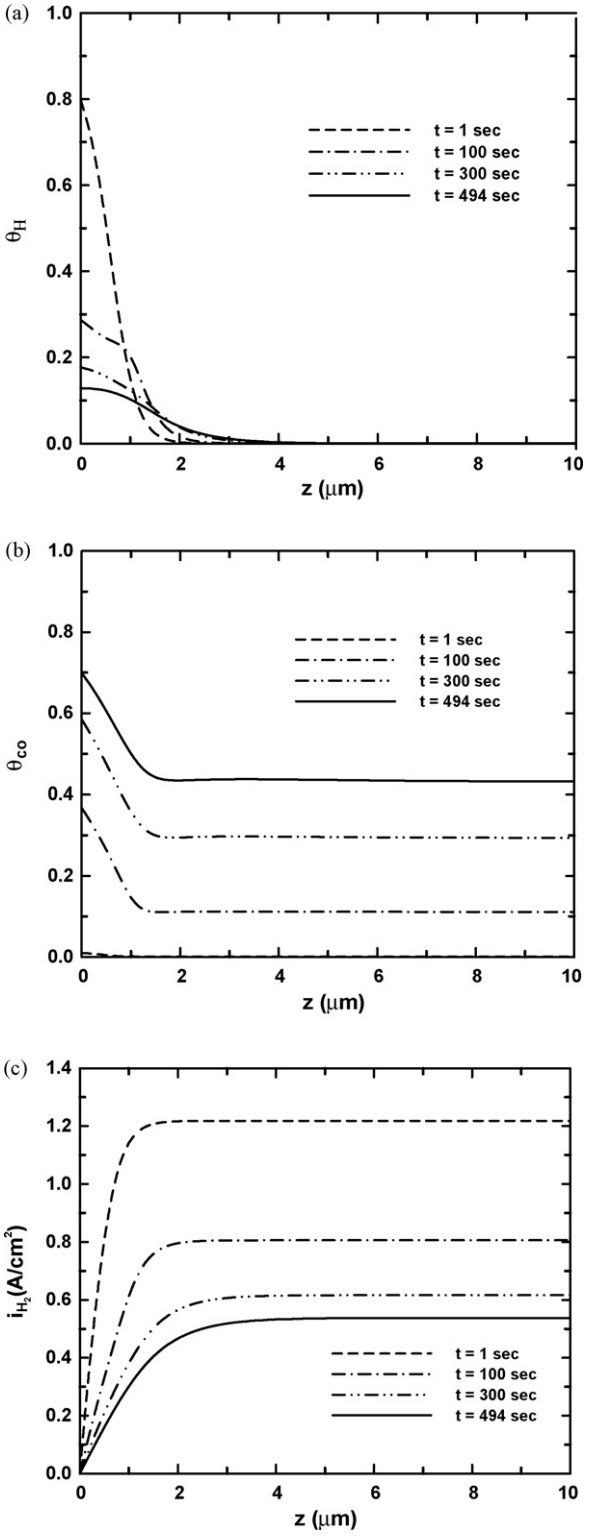

Fig. 8. Transient evolutions of (a) H_2 coverage profile, (b) CO coverage profile, and (c) current density distribution induced by H_2 under the conditions of $P_H = 0.75$ atm, $P_{CO_2} = 0.25$ atm, and 20 ppm CO.

close examination of Fig. 8 discloses that at the initial transient ($t < 1$ s), the current density was not affected by poisoning and the maximum H_2 coverage was 0.8. As poisoning time elapsed, the accumulated CO coverage was getting more and more. The CO_2 poisoning effect caused H_2 coverage decreased with time and it spends about 494 s to reach the steady state. Meanwhile, H_2 coverage was

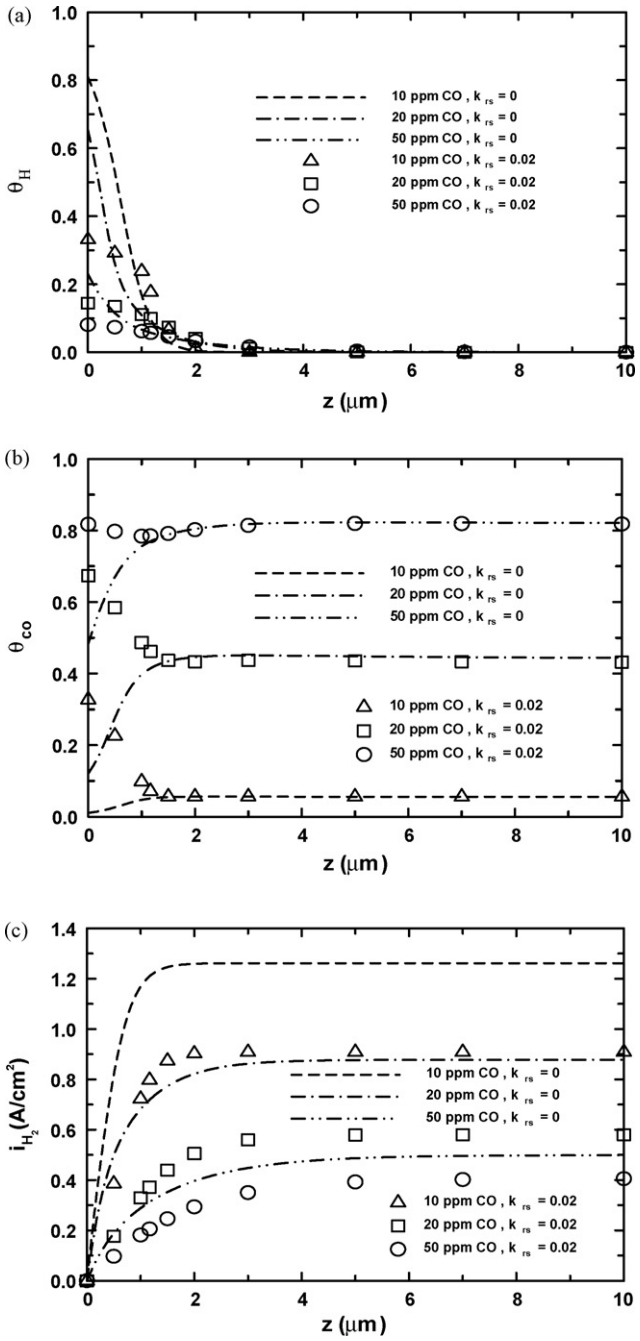

Fig. 9. Steady-state distributions of (a) H_2 coverage profile, (b) CO coverage profile, and (c) current density distribution induced by H_2 at $P_H = 0.8$ atm and $P_{CO_2} = 0.2$ atm with various CO concentrations.

only 0.12 and the current density had lowered from 1.217 A cm^{-2} to 0.537 A cm^{-2}, about 55.88% decrease. As shown in Fig. 8(b), when PEM fuel cell reached the steady state, the CO coverage got maximum value on catalyst layer surface ($z = 0$) and decreased with increasing position z.

The CO_2 poisoning effect on the PEM fuel cell depends on the rate constant of RWGS reaction k_{rs}. When k_{rs} is zero, the CO_2 poisoning effect can be neglected, otherwise the CO_2 poisoning effect should be considered. Fig. 9 presents the influence of rate constant of RWGS reaction k_{rs} on the steady-state distributions of the H_2 coverage, the CO coverage and the current density caused by H_2 in catalyst layer for various CO concentrations. An overall inspection in Fig. 9 reveals that for the conditions of the low CO concentration (10 ppm) with

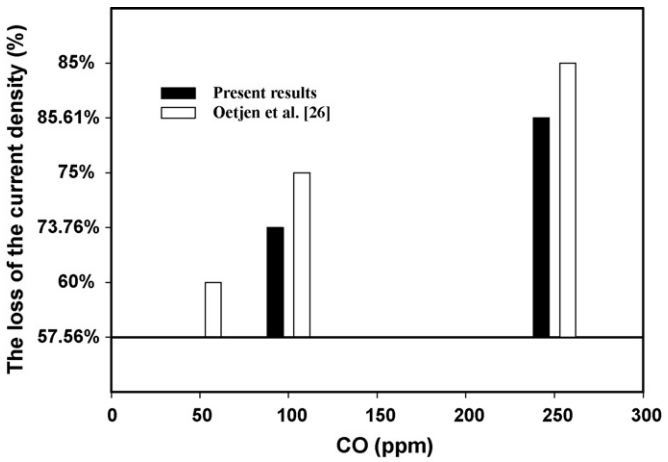

Fig. 10. Comparison of predicted current density loss with experimental data [26] under various CO concentrations.

CO_2 poisoning effects, the H_2 coverage decreased from 0.81 to 0.33 and the current density dropped from 1.262 A cm^{-2} to 0.908 A cm^{-2}. Nevertheless, for high CO concentration conditions, CO_2 poisoning has a little effect on H_2 coverage and current density of fuel cell. This is due to the fact that the platinum catalyst layer surface would be occupied by CO for high CO concentration condition, therefore, there are not enough Pt–H for CO_2 to conduct reverse water gas shift reaction.

Fig. 10 shows the comparisons between present simulated results and the experimental data [26]. In this plot, only CO poisoning was considered. The comparison shows a good agreement under various CO concentrations. At 50 ppm CO, the current density drops almost 58%. While CO concentration increases up to 100 ppm, more than 73% of performance loss is found from both prediction and experiment.

5. Conclusion

The present work mainly focuses on degradation of cell performance of PEM fuel cell at transient time due to CO and CO_2 poisoning. According to the predicted results, the following conclusions can be made:

1. The results showed that the higher CO concentration, the greater drop of cell performance.
2. When CO concentration is 0 ppm and CO_2 pressure is 10% and 40%, the cell performance decreases 24.69% and 54.6%, respectively.
3. The CO_2 poisoning became much more significantly when the CO content in the reactant gas was small.
4. At low current density conditions, CO_2 poisoning becomes much more significant. The effect of RWGS reaction reduces as current density increases.

Acknowledgement

The authors would like to acknowledge the financial support of this work by the National Science Council, R.O.C. through the contract NSC97-2212-E-211-001.

References

[1] J. Zhang, R. Datta, J. Electrochem. Soc. 149 (2002) A1423–A1431.
[2] J. Divisek, H.F. Oetjen, V. Peinecke, V. Schmidt, U. Stimming, Electrochim. Acta 43 (1998) 3811–3815.
[3] S. Gottesfeld, J. Pafford, J. Electrochem. Soc. 135 (1988) 2651–2652.

[4] H.A. Gastiger, N. Markovic, P.N. Ross, E.J. Cairns, J. Phys. Chem. 98 (1994) 617–625.
[5] H.M. Yu, Z.J. Hou, B.L. Yi, Z.Y. Lin, J. Power Sources 105 (2002) 52–57.
[6] E.I. Santiago, V.A. Paganin, M.D. Carmo, E.R. Gonzalez, E.A. Ticianelli, J. Electroanal. Chem. 575 (2005) 53–60.
[7] R.J. Bellows, E. Marucchi-Soos, R.P. Reynolds, Electrochem. Solid-State Lett. 1 (1998) 69–70.
[8] V.M. Schmidt, J.L. Rodriguez, E. Pastor, J. Electrochem. Soc. 148 (2001) A293–A298.
[9] G. Lorenz, G.G. Scherer, A. Wokaun, Phys. Chem. 3 (2001) 325–329.
[10] X. Li, J.J. Baschuk, Int. J. Energy Res. 27 (2003) 1095–1116.
[11] P.A. Adcock, S.V. Pacheco, K.M. Norman, F.A. Uribe, J. Electrochem. Soc. 152 (2005) A459–A466.
[12] A.H. Thomason, T.R. Lalk, A.J. Appleby, J. Power Sources 135 (2004) 204–211.
[13] L.P.L. Carrete, K.A. Friedrich, M. Hubel, U. Stimming, Phys. Chem. 3 (2001) 320–324.
[14] W.A. Adams, J. Blair, K.R. Bullock, C.L. Gardner, J. Power Sources 145 (2005) 55–61.
[15] T.E. Springer, T. Rockward, T.A. Zawodzinski, S. Gottesfeld, J. Electrochem. Soc. 148 (2001) A11–A23.
[16] S.H. Chan, S.K. Goh, S.P. Jiang, Electrochim. Acta 48 (2003) 1905–1919.
[17] K.K. Bhatia, C.Y. Wang, Electrochim. Acta 49 (2004) 2333–2341.
[18] H.T. Liu, T. Zhou, J. Power Sources 138 (2004) 101–110.
[19] C.P. Wang, H.S. Chu, J. Power Sources 159 (2006) 1025–1033.
[20] C.P. Wang, H.S. Chu, Y.Y. Yan, K.L. Hsueh, J. Power Sources 170 (2007) 235–241.
[21] F.A. Bruijn, D.C. Papageorgopoulos, E.F. Sitters, G.J.M. Janssen, J. Power Sources 110 (2002) 117–124.
[22] G.J.M. Janssen, J. Power Sources 136 (2004) 45–54.
[23] H. Dhar, L. Christner, A. Kush, J. Electrochem. Soc. 134 (1987) 3021–3026.
[24] M.S. Batista, E.I. Santiago, E.M. Assaf, E.A. Ticianelli, J. Power Sources 145 (2005) 50–54.
[25] S.L. Lee, Int. J. Heat Mass Transfer 32 (1989) 2065–2073.
[26] H.F. Oetjen, V.M. Schmit, U. Stimming, F. Trila, J. Electrochem. Soc. 143 (1996) 3838–3842.